Dynamic measurements of the platelet membrane glycoprotein II_b-III_a receptor for fibrinogen by flow cytometry

I. Methodology, theory and results for two distinct activators

Mony Frojmovic,* Truman Wong,* and Theo van de Ven‡
Departments of *Physiology and ‡Chemistry, McGill University, Montreal, Canada H3G 1Y6

ABSTRACT Platelet aggregation, which occurs within seconds of activation, is generally considered to be mediated by fibrinogen binding to glycoprotein II_b-III_a which becomes expressed as a fibrinogen receptor (FbR) on the activated platelet surface. This receptor expression has, however, only been measured to date at relatively long activation times (> 15 min). We have therefore developed a theoretical and experimental approach for determining FbR expression within seconds of platelet activation using flow cytometry. The fluorescently labeled IgM monoclonal antibody FITC-PAC1, was used to report on the $GPII_b$-III_a receptor for Fb (FbR). Human citrated platelet-rich plasma (PRP; diluted 1:10) was incubated with adenosine diphosphate (ADP) or phorbol myristate acetate (PMA) for varying times (τ = 0–10 s, out to 60 min), followed by incubation with fluorescein isothiocyanate (FITC)-PAC1 antibody at saturating concentrations. The time course of FITC-PAC1 binding was then measured for these variously preactivated samples (different τ) from the mean platelet-bound fluorescence (Fl), determined for $\geq$5 s of PAC1 addition by dilution quenching and determination of fluorescence intensity histograms with the FACSTAR or FACSCAN (Becton-Dickinson Canada, Mississauga, Ontario) flow cytometers. Both rapid, initial rate of increase in Fl (v) (related to PAC1 on-rates) and maximal extent of increase (Fl_{max}) were thus determined for different τ values. These measurements yield the rate of formation of FbR (k_1), and both the rate (k_2) and efficiency (α) of binding of PAC1 to FbR as a function of activator type and time of action. We have found that ADP appears to cause rapid, maximal expression of FbR within 1–3 s (k_1 > 20 min^{-1}), whereas PMA expresses FbR in a slow, biphasic manner (k_1 – 0.01 and 0.2 min^{-1}). However, k_2 and α for maximal PMA activation are about two and three times greater, respectively, than for maximal ADP-activation. Moreover, k_2 decreases with post ADP activation time. These differences are discussed in terms of altered FbR organization and accessibility. This kinetic approach can be widely used to analyze the dynamics and organization of molecules on cell surfaces by flow cytometry, including studies of size-dependent subpopulations (see Part II, Frojmovic, M., and T. Wong. 1991. *Biophys. J.* 59:828–837).

INTRODUCTION

Platelet aggregation is generally mediated by fibrinogen (Fb)[1] (1–4) which can specifically bind to the platelet membrane $GPII_b$-III_a complex (1–7). However, this complex must be transformed into a receptor for Fb (FbR) via platelet activation which alters the $GPII_b$-III_a conformation and/or its microenvironment in the membrane (3–5, 8). In this regard, the monoclonal antibody PAC1 is an IgM antibody that binds only to this activated form of the $GPII_b$-III_a complex (5, 6). This antibody probe has been shown to recognize an epitope on the II_b-III_a complex which is critical for Fb binding and to contain an arginine-glycine-aspartate-serine (RGDS) binding site (9) characteristic of adhesive molecules (Fb, fibronectin [Fn] and von Willebrand factor VIII [VWF]) (4, 7) which can all bind to the transformed $GPII_b$-III_a, typical of members of the integrin family (3, 7). In plasma, it appears that Fb is the most effective adhesive molecule for binding to the transformed $GPII_b$-III_a, which can then mediate aggregation (1, 4).

Unactivated platelets each contain ~50,000 copies of $GPII_b$-III_a which are uniformly distributed over the platelet surface. Platelet activation causes shape change, expression of newly transformed $GPII_b$-III_a which can then bind Fb, and ensuing aggregation (shown schematically in Fig. 1). Newly expressed $GPII_b$-III_a (FbR) on

Address reprint requests to Dr. M. M. Frojmovic, Department of Physiology, McGill University, 3655 Drummond Street, Montreal, Quebec, Canada H3G 1Y6.

Presented in part at the 12th International Congress of Thrombosis and Hemostasis, Tokyo, August, 1989.

[1] *Abbreviations listed in this paper:* ADP: adenosine diphosphate; F:P: fluorescein:protein ratio in molar; FA: formaldehyde; Fb, FbR: fibrinogen and receptor for Fb; FITC-PAC1: fluorescein isothiocyanate (FITC)-PAC1 antibody; Fl, Fl_{max}: mean fluorescence for a platelet population and maximal Fl at equilibrium binding, respectively; Fn: fibronectin; FSC: forward scatter; GA: glutaraldehyde; L: large platelets (~top 20%); PMA: phorbol myristate acetate; PRP: platelet rich plasma RGDS: arginine-glycine-aspartate-serine; R. T.: room temperature; S: small platelets (~bottom 20%); SSC: side scatter; t: total platelet activation time and/or incubation time of FITC antibody with platelets; τ: activation time of platelets preceding addition of FITC-antibody; v_τ: initial rate of increase in Fl for a preactivation time τ, related to initial on-rate; VWF: von Willebrand factor.

0006-3495/91/04/815/13 $2.00

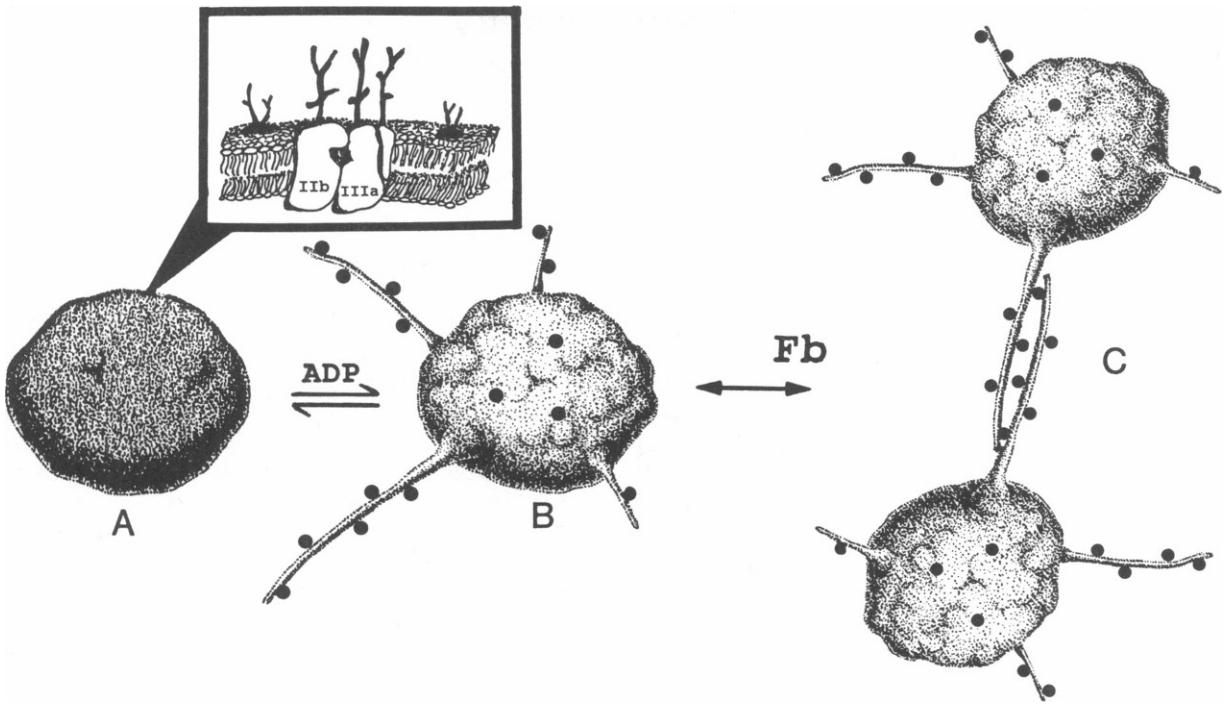

FIGURE 1 Schematic for platelet activation and expression of fibrinogen receptors. The resting platelet is a smooth discocyte (*A*) containing ~50,000 copies of glycoprotein II_b-III_a in the surface membrane (*inset*). Activation causes shape change (*B*) and "transformation" of these glycoproteins into FbR, (●) which can bind fibrinogen and allow platelet doublet and multiplet formation (*C*) occurring by 1 s after ADP addition (14, 15). The arrangement of FbR and selection of platelet contacts is only hypothetical.

the surface of activated platelets have been reported to vary from ~10,000 to 80,000 receptors, with low estimates for weak activators like adenosine diphosphate (ADP) and highest ones for strong activators like thrombin or phorbol myristate acetate (PMA) (4, 10). It appears that activators such as PMA, but not ADP, can recruit a new pool of $GPII_b$-III_a receptors from α-granules (4, 11). Finally, events after Fb binding are needed to allow its functional expression in eliciting platelet–platelet aggregation, likely related to (*a*) the increased association of $GPII_b$-III_a with cytoskeleton (1, 4); (*b*) further conformational changes occurring in $GPII_b$-III_a after binding of the Fb (7, 12), and (*c*) clustering of the $GPII_b$-III_a receptors into patches after Fb binding (2, 4, 13).

Although enormous progress has been made in the biochemistry of platelet activation and of the platelet membrane $GPII_b$-III_a, very little is known of the dynamics of expression of the FbR and of its relation to the dynamics of platelet aggregation. Platelets activated with ADP immediately begin to change shape ($\ll 1$ s), and after a delay of ~1 s, single platelets are maximally recruited into microaggregates by 8–10 s with a half-time of ~3 s (14, 15). This is summarized schematically in Fig. 1. We therefore wished to determine the dynamics of expression of the transformed $GPII_b$-III_a receptor for Fb on such shape-changed platelets (Fig. 1) between 0 and 10 s of ADP activation, and to determine any changes occurring in "steric accessibility" of this FbR with increasing activation time. We hypothesized that we might find a continuous expression of FbR between 1 and 10 s at the rate of >1,000 new sites expressed per second (4, 10).

The probe chosen for these kinetic studies was PAC1. Such rapid measurements could not be made with traditional radiolabeled probes (1, 4, 10). We therefore chose to use fluorescently labeled PAC1 and flow cytometry (6), with PAC1 suited for studies in platelet-rich plasma (PRP) as it readily displaces reversibly bound Fb (6). We developed a rapid dilution quenching protocol and appropriate theoretical treatments to assess the rapid expression and dynamic changes in FbR. This approach has yielded a novel general technique for assessing the rapid dynamics of any cell surface molecule as well as unexpected new insights into the kinetic expression and nature of FbR formed on platelet surfaces activated with ADP and PMA.

MATERIALS AND METHODS

Processing of PRP for activation and flow cytometric measurements

Venous blood was obtained from healthy human donors who were not on any medication. Whole blood (9 vol) was anticoagulated with 3.8% sodium citrate (1 vol) and was centrifuged at 150 *g* for 15 min at room temperature to obtain PRP. The PRP was then incubated at 37°C for 30 min and an aliquot was tested for aggregation in response to activator addition (typically, 0.2 μM PMA and 10–100 μM ADP by turbidimetry [15]). The PRP was diluted 10-fold by the addition of prewarmed (37°C) Walsh-albumin buffer (modified Tyrodes buffer (NaCl 140 mM, KCl 2.7 mM, $NaHCO_3$ 0.4 mM; pH 7.4) containing 0.1% glucose, 0.2 mM $MgCl_2$, and 0.1% bovine serum albumin) to obtain PRP 1:10 as described by Shattil et al. (6). It was further incubated at room temperature (R.T.) for 15 min.

Unless otherwise stated, each sample for flow cytometric measurement consisted of 22.5 μl of PRP 1:10, plus 2.5 μl of activator (100 μM ADP or 0.2 μM PMA) added at R.T. to 12 × 75 mm polystyrene tubes for varying incubation times (τ) before the addition of fluoroscein isothiocyanate (FITC)-antibody (4.5–5.5 μl). These activator concentrations were chosen to ensure maximal responses in all PRP samples. Mixing was routinely done by rapid hand-swirling, for < 1 s, to ensure complete mixing of reagents but negligible aggregation during the 1 s latent time reported for samples stirred in a cuvette; the extent of platelet aggregation was determined by microscopy (14).

Optimal times τ of activation yielding maximal rates of PAC binding site expression were found to be ≪ 10 s and > 25 min for ADP and PMA, respectively. For τ > 25 min for PMA, > 100 μl of PRP (1:10) was preactivated with PMA, and 25 μl aliquots were then used for FITC-PAC1 binding studies, with no differences observed for τ varying between 25 and 60 min. Incubation time (t) of the PRP (1:10) (± activator) with FITC-antibody was varied from 5 s to 60 min before the addition of Walsh buffer (10 vol) to quench-dilute the reaction mixture. A few samples were prepared for live measurements in the flow cytometer (no dilution), using > 4 vol of PRP (1:10) (90 μl) and the same final concentrations of activator and antibody (116 μl final vol). The final concentration of FITC-antibody in PRP (1:10) was chosen so as to give saturation conditions ensuring > 90% of maximal fluorescence values after > 30 min binding to maximally activated platelets as previously described (6); this was ~25 and 40 μg/ml (±10%) for the two different preparations used (fluorescein:protein [F:P] ratios were respectively 7.7 and 7.0).

Fixation experiments

In preliminary experiments, our primary strategy was to fix platelets with aldehyde in order to trap and arrest the formation of new FITC-PAC1 binding sites at very early activation times with ADP (< 10 s) without causing destruction of these new sites as reported for 1% formaldehyde fixation (6). We found that addition of as little as 0.15% formaldehyde (FA) or 0.10% FA plus 0.05% glutaraldehyde (GA) (4 vol) to control PRP (undiluted) at 37°C for 30 min could (*a*) prevent any activation associated with platelet shape change, and (*b*) did not yield enhancement in autofluorescence seen with > 0.5% GA fixation. However, such fixation of PRP preactivated with 100 μM ADP or 0.2 μM PMA (τ = 15 and 25 min, respectively) caused 70% reduction (50–80% for six donors evaluated) in maximal Fl at equilibrium binding (Fl_{max}) compared to nonfixed samples; fixed platelets were diluted 1:10 as above for flow cytometry. Moreover, fixation alone caused > 5% of Fl_{max} to be expressed when excess fixative was neutralized with < 0.1 M glycine (final concentration) added 3 s after fixative addition, a modification of a procedure reported by George et al. (16). This is an underestimate of "activation" given major "disappearance" of Fl_{max} above. Pelleting and washing of platelets after fixation, or use of glycine, or studies with washed platelets freed of plasma proteins by pelleting and resuspension (16) did not alter the spontaneous activation and major destruction of FITC-PAC1 binding sites.

Flow cytometry measurements

The platelet samples were analyzed for 2,500–5,000 cells in a FASCSTAR or FACSCAN flow cytometer (Becton-Dickinson Canada, Mississauga, Ontario). Light scatter and fluorescence data (forward scatter [FSC], side scatter [SSC], and one color fluorescence [Fl1]) were obtained with flow cytometer gain settings in the logarithmic mode and analyzed with Becton-Dickinson Canada C30 software on a model 300 computer (Hewlett-Packard Co, Palo Alto, CA) to yield dual parameter dot plots, single parameter histograms, or mean values. Comparable results were obtained with the two flow cytometers, with values ~50% greater with the FACSTAR than with the FACSCAN (Becton-Dickinson Canada). Platelets were distinguished from background/cellular debris and electronic noise on the basis of forward and side scatter dot plots by setting a lower FSC threshold to exclude the background during data acquisition, as previously reported (6). These dual parameter dot plots, shown as contour plots (contour level set at a minimum of five points) (Fig. 2 *A*) were distinct for control PRP or PRP maximally preactivated with ADP or PMA, but rectangular gates were set to enclose the complete contour plots (Fig. 2 *A*) (this included > 95% of all particles acquired above the lower threshold). The fluorescence histograms for these gated populations were then obtained (Fig. 2 *B*); gates were set to include the entire histogram, typically between 1.1 and 5,000 fluorescence units for all samples (Fig. 2 *B*); mean and mode fluorescence values were determined with the Becton-Dickenson Canada C30 software which obtains the linear channel numbers, determines the average values, and then converts to mean log channel number (for a fixed 64 channels per decade). For both unactivated and maximally activated platelets, after > 30 min of FITC-PAC1 binding to the platelets, the mean and mode values for fluorescence (Fl) and FSC for a platelet population were within < 5% of each other due to the symmetrical shapes of the histograms. Mean values of Fl are reported. Unless otherwise shown, Fl values associated with FITC-PAC1 binding to activated platelets

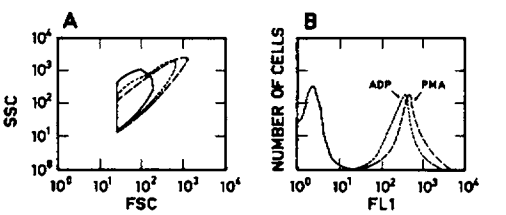

FIGURE 2 Detection of platelets and measurement of fluorescence histograms for FITC-PAC1 binding to platelets. The dot plots of SSC and FSC (*A*) and the fluorescence histograms of the gated platelets (*B*) are shown for control PRP (—), and for PRP preactivated with 100 μM ADP for 15 min (τ = 15 min) (- - -) or with 0.2 μM PMA for 25 min (τ = 25 min) (- - -). The samples were incubated with FITC-PAC1 for 30 min (t = 30 min) representing the time for maximal binding, and quench diluted just before analysis (see Methods). Mean FSC was 77, 92, and 102, respectively, for control, ADP- and PMA-treated platelets.

have been corrected for background binding by subtraction of Fl values for FITC-PAC1 binding in the absence of activator.

For dilution-quenched samples, flow cytometry data were routinely collected within 30–60 s of dilution quenching to minimize any postdilution time-dependent changes. Fl_{max} values so measured for PRP maximally preactivated with PMA (τ = 25 min) and incubated with FITC-PAC1 for >30 min before dilution, did not significantly change between 30 s and 5 min. Live measurements with PRP (1:10) containing FITC-PAC1 (with no further dilution) were made over a 10 s interval, with the mean value (t) used for Fl versus t plots (e.g., t = 10–20 s for data collection, t = 15 s) (Fig. 3 *A*). No significant differences were observed in Fl versus t for quench-diluted (observed <60 s postdilution) versus live experiments conducted in parallel for early binding times of FITC-PAC1 to maximally preactivated platelets (Fig. 3 *A*). Similarly, no significant off-rate was observed for preactivated samples dilution quenched after 5, 15, or 30 s incubation with FITC-PAC1 when followed in real time between 15 and 120 s postdilution. The <15% apparent increase in Fl which could occur due to significant on-rates over the 0 s postdilution (Fig. 3 *B*) is, however, within the reproducibility of any one measurement. Thus, triplicate measurements of Fl at various time points shown in Fig. 3 *A* made for six donors gave standard deviations in mean values of ±15% (range 2–33%) for both live and quench-diluted samples.

Monoclonal antibodies

PAC1, a murine monoclonal antibody having specificity for activated glycoprotein II_b-III_a (6), was generously provided by Dr. Sanford Shattil (University of Pennsylvania, PA) (5, 6). FITC conjugation of PAC1 was done as previously described (6); aliquoted stocks of this material were stored at −70°C, freshly thawed on the day of use, and spun for 5 min at 8,700 *g* to remove antibody aggregates. The F:P molar ratio was 7.7 and 7.0 for two different preparations for the FITC-PAC1. Human hybridoma IgM (lupus anticoagulant) antibodies used to test the nonspecific binding of IgM to platelets (see Fig. 5) were generously provided by Dr. J. Rauch (Montreal General Hospital, Montreal, Canada): the B110 and B111 which did not bind to phospholipids, and 9604 which did (17); FITC labeling procedure and F:P ratios were as for the PAC1.

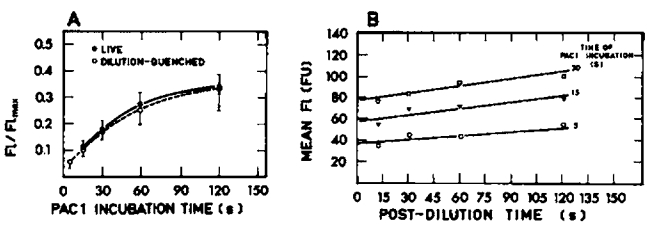

FIGURE 3 Effect of dilution quenching on the measured binding of FITC-PAC1 to activated platelets. The time course of Fl associated with platelets preactivated with 0.2 μM PMA (τ = 25 min) is compared for (*A*) live samples measured in real time with no dilution versus dilution-quenched samples measured between 30 and 60 s postdilution for FITC-PAC1 binding times (t) of 15–60 s, and (*B*) dilution-quenched samples as a function of time postdilution, for FITC-PAC1 binding times of 5, 15, and 30 s preceding dilution quenching. In (*A*), 1 and 4 vol of PRP (1:10) + FITC-PAC1 were used for dilution quenched and live samples, respectively, with t reported as the mean of the time needed to collect in real time (see Methods). The Fl values were normalized to Fl_{max} obtained at t = 30 min; data are for three experiments, with bars = ±1 SD. In (*B*) data are for one donor; regression lines are best-linear fits having correlation coefficients of 0.88, 0.85, and 0.92, respectively for t = 5, 15, and 30 s ($p < 0.1$ for three lines). The line has been back-extrapolated to zero time intercepts.

Materials and chemicals

All chemicals and reagents, unless otherwise specified, were purchased from Sigma Chemical Co. (St. Louis, MO). Platelet activators ADP and PMA were diluted in Walsh buffer from respective stocks of 0.02 M (in Tyrode's pH 7.4) and 1.6 mM (in 100% ethanol) stored at −20°C. Vehicle additions of activator to 10-fold diluted platelet-rich plasma were <10% (vol/vol). Fluorescein isothiocyanate (FITC; Isomer I, on celite 10%) used for monoclonal antibody labeling was purchased from Behring Diagnostics (La Jolla, CA). Aldehyde solutions used for platelet fixation were freshly prepared as previously described from solid paraformaldehyde (Fisher Scientific, Montreal, Canada) and 8% glutaraldehyde solution in sealed ampoules (Polysciences Inc., Warrington, PA).

THEORY

Consider unactivated platelets (P) converted to activated platelets (P*) after addition of an activator:

$$P \underset{k_{-1}}{\overset{k_1}{\rightleftharpoons}} P^*. \tag{1a}$$

New sites will be expressed for fibrinogen binding per unit area of membrane surface (n) at a rate k_1:

$$\frac{dn}{d\tau} = k_1 (n_{max} - n) - k_{-1} n. \tag{1b}$$

Here, n_{max} is the maximum number of sites which can be activated, i.e., the maximum number of receptors expressed (FbR or PAC1-binding sites formed); k_{-1} is the rate at which sites are deactivated, and τ is the time of activation.

The solution of Eq. 1 when k_1 and k_{-1} are constant is

$$n = \frac{k_1}{k^*} n_{max} (1 - e^{-k^* \tau}), \tag{2a}$$

where $k^* = k_1 + k_{-1}$. For short times ($\tau \to 0$)

$$\frac{d(n/n_{max})}{d\tau} = k_1, \tag{2b}$$

and hence,

$$n = n_{max} k_1 \tau. \tag{2c}$$

Addition of a fluorescently labeled monoclonal antibody at an initial concentration m_o (number of molecules per unit volume) will yield binding of the marker

molecules to activated sites at a rate k_2:

$$\frac{dm_s}{dt} = k_2 m_o (1 - A_p m_s/m_o)(n - m_s). \quad (3)$$

Here m_s is the number of marker molecules per unit area which are bound to the activated sites; m_o $(1 - A_p \cdot m_s/m_o) = m$ is the number of marker molecules per unit volume in solution at time t, A_p being the total platelet area per unit volume, and $(n - m_s)$ is the number of unoccupied activated sites per unit area.

Now consider the following three conditions: (*a*) when activator and marker molecules (PAC1) are added together, so that at $t = 0, n = 0$, the solution of Eq. 3 for short times ($t \to 0$) is:

$$m_s = \tfrac{1}{2} k_1 k_2 m_o n_{max} t^2. \quad (4)$$

Eq. 4, together with the fact that $m_s \to n_{max}$ as $t \to \infty$, predicts that a plot of m_s versus time t will be S-shaped. (*b*) When excess marker molecules are used ($m_o \gg n_{max}$), which are added after preactivation of the platelets for a time τ, Eq. 3 reduces for short times to

$$m_s = k_2 m_o n_\tau t, \quad (5)$$

where n_τ is the number of activated sites at time $t = 0$ (before marker molecule addition). With no preactivation, $n_\tau = 0$ and Eq. 4 applies. Eq. 5 shows that when the sites are preactivated, the number of marker molecules binding to the activated sites is initially a linear function of time, as well as a function of n_τ.

Now, consider a fluorescently labeled probe such as FITC-PAC1 which binds specifically to new receptor sites where the mean fluorescence of bound molecules (Fl) is a linear function of the actual number of bound molecules (m_s) (6), i.e.,

$$m_s = c' \mathrm{Fl}, \quad (6)$$

where c' = a constant relating Fl to actual numbers of molecules, determined by the instrument and settings chosen, and by the degree of labeling of the FITC-PAC1 (the F:P ratio [6]). It follows that the rate of increase in Fl due to binding of FITC-PAC1 added at time τ after platelet activation is

$$v_\tau = \frac{d\mathrm{Fl}}{dt} = \frac{1}{c'} \frac{dm_s}{dt}. \quad (7a)$$

Combining Eqs. 5 and 7, we obtain for short times

$$v_\tau = (k_2 m_o/c') n_\tau. \quad (7b)$$

A. Experimental procedure for determining k_1

It follows from Eq. 7 that v_τ will increase in direct proportion to the number of new sites, n_τ, present at the time τ of addition of FITC-PAC1. Considering maximal activation associated with v_{max} and n_{max}, we have

$$v_\tau/v_{max} = n_\tau/n_{max}, \quad (8)$$

for constant k_2, and using Eq. 2, we obtain for short times

$$\frac{d(v_\tau/v_{max})}{d\tau} = k_1. \quad (9a)$$

At longer τ times (rewriting Eq. 1b with $k_{-1} = 0$),

$$\frac{d(v_\tau/v_{max})}{d\tau} = k_1 (1 - v_\tau/v_{max}). \quad (9b)$$

Thus, a plot of v_τ/v_{max} against τ will yield the rate of expression of new PAC1-binding sites or FbR sites (k_1) at early and later times of activation.

B. Experimental procedure for determining $k_2 m_o$

In the case where τ is chosen so that *maximal expression* of new receptors has occurred before addition of marker molecule, Eq. 8 becomes

$$v_{max} = \frac{k_2 m_o}{c'} n_{max} = (k_2 m_o)\, \mathrm{Fl}_{max}, \quad (10)$$

where k_2 is the rate constant for the binding of marker molecules to already expressed receptors, unchanging in time, and $n_{max} = m_{max}$ (i.e., PAC1 has a 1:1 stoichiometry with FbR at early times). Eq. 10 applies only when $k_{-1} = 0$, i.e., no deactivation of PAC1 binding sites occurs. Otherwise, n_{max} in Eq. 10 must be replaced by $(k_1/k^*)n_{max}$. It follows from Eq. 10 that $k_2 m_o$ is directly obtained from $v_{max}/\mathrm{Fl}_{max}$ for maximally preactivated platelets.

(*c*) Finally, we must consider that rate constants (k) may change dynamically in time or be distinct for different activators due to (1) a change in the source or properties of the receptor (k_1 or k_2 affected), (2) dynamic "disappearance" of the receptor with time (k_{-1} component), and (3) time-dependent steric changes in accessibility of the receptor sites by the marker molecule m (FITC-PAC1) (k_2). In this case, Eq. 3 must be solved in conjunction with Eq. 1b in which k_1, k_{-1}, and k_2 are time dependent. However, for condition 2 above,

$$(v_\tau)_{t \to 0} = k_2(\tau)\, m_o\, n_\tau, \quad (11)$$

where $k_2(\tau)$ is the value of k_2 at time $t \to 0$ for varying preactivation times τ. $k_2(\tau)$ may vary due to activation-

dependent changes in receptor's microenvironment or surface organization (e.g., clustering).

Efficiency of PAC1 binding

From the conservation of marker molecules (i.e., the number of marker molecules disappearing from solution equals the number of molecules adsorbing onto platelets), it can be shown that the efficiency α with which marker molecules colliding with platelets are captured by them, is given by

$$\alpha = \frac{k_2}{k_{sm}} S. \tag{12}$$

Here α is the number of collisions between marker molecules and platelets leading to capture (adsorption), divided by the total number of such collisions; S is the number of binding sites per platelet, and k_{sm} is the rate constant for the disappearance of marker molecules from solution, as calculated from classical Smoluchowski kinetics (18), assuming platelets and marker molecules can be modeled as effective spheres of radius a_{pl} and a_m respectively. When $a_{pl} \gg a_m$,

$$k_{sm} = 2\pi D_m \frac{a_{pl}}{a_m} = \frac{kT}{3\eta} \frac{a_{pl}}{a_m}. \tag{13}$$

Here D_m is the diffusion constant of a marker molecule, k is Boltzman's constant, T the absolute temperature, and η the viscosity of the medium. At room temperature, $T = 398°K$; in water, $\eta = 1$ mPas, and taking $a_{pl} \sim 1$ μm (18) and $a_m \sim 30$ nm (20), yields $k_{sm} \sim 5.10^{-17}$ $m^3 s^{-1}$.

From Eq. 12 it can be seen that from a measurement of k_2 and a knowledge of the number of sites, the efficiency α can be determined. Relative α values are obtained, for a given platelet preparation but for two different activators, by

$$\alpha_1/\alpha_2 = V_{max1}/V_{max2} \tag{14}$$

obtained by combining Eqs. 10 and 12 and having $n_{max} = S$.

RESULTS

Methods of "trapping" FITC-PAC1 bound to platelets

Previous investigators have studied the binding of FITC-PAC1 to platelets maximally activated with ADP or PMA by incubating platelets with both activator and antibody, and obtaining Fl values near equilibrium conditions for maximal binding (>15 min) (5, 6). We wanted to obtain Fl values as a function of the duration of platelet preactivation (τ), as well as for very early times of incubation ($t < 5$ s) of platelets with the FITC-PAC1 marker. Our theoretical model above predicted that such an approach would yield new information on both the rate and extent of appearance of new PAC1 binding sites which represents the expression of new FbR. This approach therefore required rapid data acquisition from PRP for times $t < 5$ s, given that platelet aggregation, believed to require FbR, occurs within 1 s of activation with >2 μM ADP, with 50% of single platelets recruited by ~3 s (Fig. 1) (14, 15).

Our first strategy was to quench FbR expression by fixing platelets with aldehyde within 1–10 s of reaction with 100 μM ADP and then incubating with FITC-PAC1 for varying times t. However, this approach had to be abandoned as the FITC-PAC1 binding site (transformed $GPII_b$-III_a) appeared to become largely denatured for the wide spectrum of fixation and "clean-up" conditions explored as previously reported by Shattil et al. for 1% formaldehyde fixation (6) (see Methods). Fortunately, it was found that a simple 10-fold dilution quenching of the PRP reaction mixture, and analysis with the flow cytometer, within 60 s of dilution allowed a measure of the fluorescence histogram and Fl values corresponding to the precise time t at which the PRP ± activator + FITC-PAC1 was dilution quenched. This approach allowed significant Fl values to be measured as early as 5 s after addition of FITC-PAC1 to PRP (1:10) samples (see Methods and Fig. 3). For PAC1 incubation times t > 15–30 s, live experiments without dilution quenching were equivalent to dilution-quenched experiments (Methods and Fig. 3 *A*), but the former requires at least four times more PRP and antibody for any one experiment. We therefore have chosen the dilution-quench approach as the most efficient technique.

Extent of platelet aggregation during activation and incubation

Given that aggregates of platelets will yield artifactually high values of mean fluorescence per platelet, we made direct measurements of the extent of aggregation in representative samples fixed for flow cytometry using microscopy as previously reported (14). Control PRP 1:10 examined out to 25 min of incubation at room temperature without activator typically contained <2% of all particles as doublets, and <1% as triplets, with no higher order aggregates. This is comparable to the <4 ± 2% of all particles as aggregates in control PRP previously reported for 34 healthy donors (14). Samples of PRP 1:10 activated with ADP or PMA, as described above, contained <5% of all particles as doublets, and <1% as triplets, i.e., >95% singlets, for τ ranging from 3 s to 15 min for ADP, and from 10 to 25 min for PMA.

Given an uncertainty in aggregation of platelet samples of <5%, we have compared mean Fl values for the total platelet population versus 95% of the population with the top 5% gated out for largest FSC values: we found <8% reduction in Fl values for v, and Fl_{max} for either ADP or PMA as activators. This is clearly an overestimate, as mean FSC did not in fact significantly increase for PRP samples stirred for 3 s with 10 μM ADP to yield 20% of particles as doublets and triplets. Moreover, any effects due to aggregation are further reduced as ratios of mean Fl are used to obtain k_1 and k_2 values.

Time course of FITC-PAC1 binding to platelets by dilution quenching

For a given condition of preactivation (τ values) and incubation with FITC-PAC1 (t values), fluorescence histograms were obtained at selected t values by rapid dilution quenching and measurement of >2,500 cells. This is demonstrated in Fig. 4 using PRP incubated together with 100 μM ADP ($\tau = 0$) and FITC-PAC1 (at saturating concentrations) for t values ranging from 15 s out to 45 min of PAC1 incubation, and contrasted to unactivated PRP in the absence of PAC1 ($t = 0$). Fluorescence histograms were also obtained in parallel for unactivated PRP incubated with FITC-PAC1. Plots of Fl versus PAC1 incubation times were thus determined from such histograms, and the time course for specific Fl (corrected for nonspecific binding) was obtained as shown in Fig. 5 for platelets maximally preactivated with PMA. The slope of the initial linear rise in specific Fl yields v, whereas the maximal rise in specific Fl yields Fl_{max} (see Eq. 9).

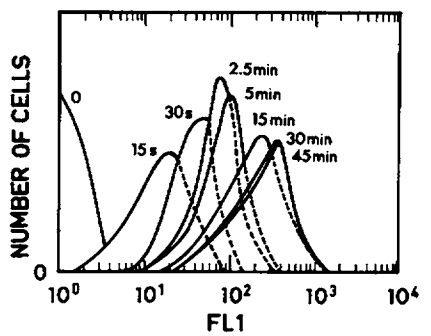

FIGURE 4 Dynamics of fluorescence histograms in activated platelets with time-dependent binding of FITC-PAC1. A fluorescence histogram is shown for unactivated PRP without FITC-PAC1 ($t = 0$). Parallel PRP samples were then incubated with 100 μM ADP and FITC-PAC1, the suspension was dilution quenched after 15 and 30 s out to 45 min, and fluorescence histograms obtained at each of these times.

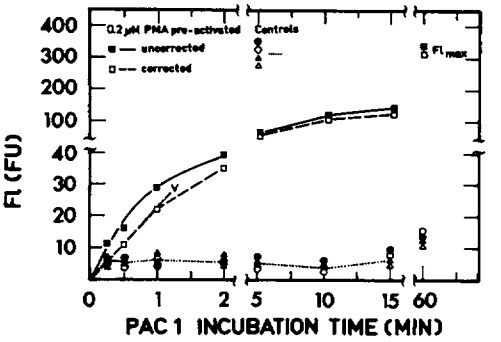

FIGURE 5 Time course of mean fluorescence associated with resting and activated platelets using FITC-PAC1, EDTA and a nonspecific IgM probe. The mean fluorescence values (Fl) were obtained for unactivated PRP (○) and for PRP maximally preactivated with 0.2 μM PMA ($\tau = 25$ min) (■) as a function of incubation time with FITC-PAC1; these were determined from histograms as shown in Fig. 3. The Fl versus t curve for PMA activated platelets (—) was then corrected for nonspecific binding by curve subtraction (- -). The initial rate of increase in Fl (v) and maximal extent, Fl_{max}, are indicated. The uncorrected Fl curves are also shown for (*a*) the above with 5 mM EDTA (●) added 1 min before PMA addition(s), and (*b*) a nonspecific IgM (B111) for control (△) and PMA activated (▲) as for PAC1. One curve (- - -) is generated to represented these four controls, PRP ± EDTA and PRP ± PMA + B111. Identical results were obtained with B110 and 9604 IgM's (see Methods).

Specificity of FITC-PAC1 binding to its fibrinogen receptor

To explore the possibility that the rapid binding of FITC-PAC1 to activated platelets (Figs. 5 and 6) arises

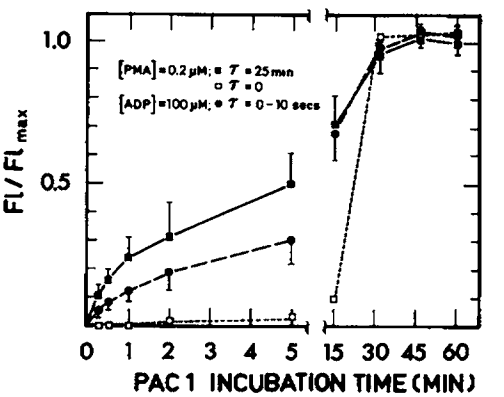

FIGURE 6 Comparison of overall kinetics of PAC1 binding to platelets activated with ADP and PMA. Corrected Fl values were obtained for platelets maximally preactivated with 0.2 μM PMA ($\tau = 25$ min; [■]) and 100 μM ADP ($\tau = 0$–10 s; [●]) as a function of FITC-PAC1 incubation time (t) for five donors for t values ranging from 15 s out to 10 min. The time course for PMA added with PAC1 ($\tau = 0$ min; [□]) is shown for one donor. Fl values are normalized by comparing to Fl_{max} values measured for $t = 45$ min, separately done for each donor and for each activator. All donors were common for both activators.

from a rapid entry into membrane compartments opening with platelet activation, quite apart from specific binding to the fibrinogen receptor $GPII_b$-III_a, we compared the binding kinetics of FITC-labeled IgM antibodies which bind nonspecifically to the platelet surface and/or to phospholipids. All three such antibodies (B110, B111, 9604) (17) showed rapid Fl saturation curves, independent of platelet activation, as shown for one of these in Fig. 5. In addition, we found that activation of platelets in the presence of 5 mM EDTA, which allows full shape change (21) but inhibits binding of both Fb and of PAC1 to the specific $GPII_b$-III_a receptor for Fb (5, 6), showed a rapid binding as seen for all other "nonspecific" binding (Fig. 5). The nonspecific binding is consistent with a dynamic equilibrium between adsorption and desorption of the antibodies with an average "residence" time of the order of 10 s.

Comparison between experimental results and theory

Condition 1

When both activator and probe are added together ($\tau = t = 0$), Eq. 4 predicts an S-shaped curve for Fl versus time for PAC1 binding to platelets, as seen in Fig. 6 for PMA at $\tau = 0$. Using Eq. 2b, we calculate k_1 for platelets activated with PMA ($\tau = 0$) from the initial slope of Fl/Fl_{max} ($V = n/n_{max}$), shown in Fig. 6 to be 10^{-2} min^{-1}. Using Eq. 10, we calculate $k_2 m_o$ for maximally preactivated platelets from the initial slope (V) = 0.4 min^{-1}. With these values of k_1 and k_2, Eq. 4 predicts reasonably the low Fl/Fl_{max} values at low t values (<5 min) for PMA added at $\tau = 0$ in Fig. 6. As Eq. 4 is only valid for short times, it is not surprising that this equation greatly overestimates values at larger t (>15 min).

Quite surprisingly, no S-shape curve was seen when 100 μM ADP was added together with FITC-PAC1 (compare Figs. 6 and 7 for $\tau = 0$ and Fig. 8 *B*). A comparison of early time points for binding of FITC-PAC1 added to platelets together with ADP ($\tau = 0$) shows rapid and significant binding by 5 s, with back-extrapolation to a zero intercept in all four donors examined (Fig. 7). These results suggest that whereas initial FbR expression with PMA activation is slow (see also Fig. 9), ADP activation expresses FbR on the platelet surface in ≪5 s of activation; this corresponds to $k_1 \gg \frac{1}{5}\ s^{-1}$ or $\gg 12\ min^{-1}$.

Rate of expression of FbR (k_1)

Condition 2A

The time courses for PAC1 binding to platelets with varying preactivation times (τ) are shown for platelets

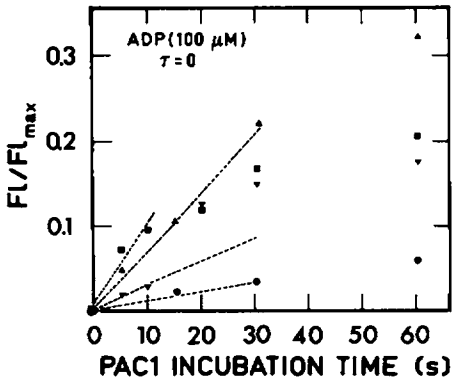

FIGURE 7 Initial rate of Fl increase for ADP added together with FITC-PAC1 ($\tau = 0$). PRP (1:10) was incubated with 100 μM ADP and FITC-PAC1 added at the same time ($\tau = 0$) and suspensions were dilution quenched at t = 5 and 10 s, out to 60 s, with Fl values obtained at each time point, as shown for four different donors. Fl values have been corrected for nonspecific binding and normalized to Fl_{max} (t = 45 min) values determined for each donor; these were 164 (▼), 175 (▲), 350 (●), and 500 (■) fluorescence units. Regression lines have been drawn from 0 Fl to the two earliest t points measured in each case to illustrate the range of initial PAC1 binding rates.

activated with PMA (Fig. 8 *A*) and ADP (Fig. 8 *B*). By plotting the initial rate of increase in specific Fl due to PAC1 binding determined from these curves (v_τ) as a function of τ, we can determine the rate of expression (k_1) of PAC1 binding sites (FbR) from the initial slope as predicted by Eq. 9a, and shown in Fig. 9. In the case of PMA activation, there appears to be a slow initial expression of FbR over the first ~10 min of activation ($k_1 \sim 0.01\ min^{-1}$; Table 1). However, for ADP activation, essentially the same initial rate of increase in Fl (v) was seen whether FITC-PAC1 was added with ADP ($\tau = 0$) or added 1, 2, or 3 s later (data shown for one of three donors so evaluated for $\tau = 0$ and 3 s in Fig. 8 *B*). This is consistent with maximal FbR expression occurring well within 3 s and a k_1 value >20 min^{-1} (Table 1).

Rate of PAC1 binding ($k_2 m_o$) for maximally preactivated platelets

Condition 2B

Eq. 9 predicts that for a fixed concentration of FITC-PAC1, $k_2 m_o$ will be constant independently of varying Fl_{max} values for qualitatively identical PAC1 binding sites: i.e., $v_{max}/Fl_{max} = k_2 m_o$ = constant. We chose platelets maximally preactivated with 0.2 μM PMA for τ = 25–30 min to test Eq. 10 because neither v_{max} nor Fl_{max} changed beyond τ = 25 min, tested out to 85 min. We first compared v_{max}/Fl_{max} values within a given PRP for distinct platelet subpopulations electronically gated

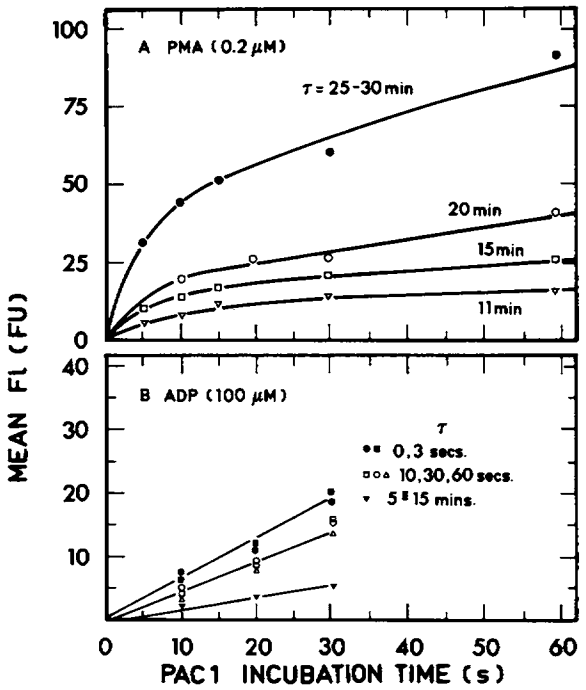

FIGURE 8 Dependence of initial rate of PAC1 binding to activated platelets on preactivation time. Corrected Fl values versus incubation time with FITC-PAC are shown for one typical donor for PRP activated at different times τ with (*A*) 0.2 μM PMA, and (*B*) 100 μM ADP. For ADP, Fl was averaged for τ = 5 or 15 min, as they were identical.

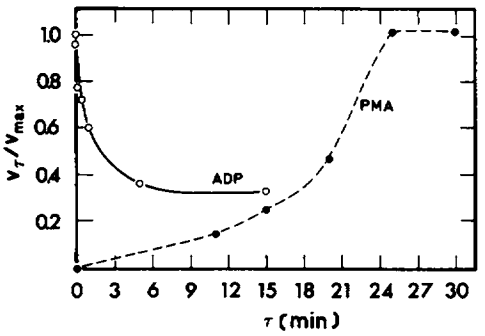

FIGURE 9 Initial rate of PAC1 binding (v_τ) as a function of platelet preactivation time (τ) for ADP and PMA. The initial rate of Fl increase (v_τ) was determined from the initial slopes of the curves shown in Fig. 8 *A* and *B* as a function of preactivation time (τ), respectively for PMA (●) and ADP (○) activation. The v_τ values are normalized to maximal values (v_{max}) obtained for $\tau > 25$ min and 0–3 s, respectively for PMA and ADP activation (data in Fig. 8). Note that $v_\tau/v_{max} = 1.0$ for ADP at the earliest time point measured ($\tau = 0, t = 5$ s), so that k_1 cannot be determined from the initial slope of v_τ/v_{max} for ADP, as it can for PMA, using Eq. 9. Note that for constant k_2, $v_\tau/v_{max} = n_\tau/n_{max}$ (cf. Eq. 8).

from the 20% of the largest forward scatterers (L) and the 20% of the smallest forward scatterers (S). These L and S platelets had distinct V_{max} and Fl_{max} values, but as predicted by Eq. 10, V_L/V_S equals Fl_L/Fl_s for each of the five donors evaluated for varying Fl_{max} values (Table 2). The ratios in the last column of Table 2 effectively represent k_2(S):k_2(L) values, which are constant.

We next compared v_{max} and Fl_{max} values for different donors for both ADP and PMA maximally preactivated PRP samples (Table 3). The mean k_2m_o values for ADP and PMA, derived from v_{max}/Fl_{max} values for m_o = 24 μg/ml PAC1, are respectively shown in Table 3. Values of k_2m_o were within 1 SD from the mean for 6 of 11 donors and 6 of 9 donors for PMA and ADP-activated platelets, respectively; the balance of donors had k_2m_o values within 1.2 SD of the mean. For the former "normal" donors, v_{max} varied linearly with Fl_{max}, with r values for a linear regression of 0.83 and 0.74, respectively, for PMA and ADP-activated platelets (figure not shown). A comparison of parameters for the same PRP preparation, done for six donors (Table 3), shows that PMA-activated platelets maximally express ~1.8 × more PAC1 binding sites (FbR) than do the ADP-activated platelets.

We can calculate the efficiency of PAC1 binding to its specific receptor sites using Eq. 12. For PMA activation $k_2m_o = 0.40\ min^{-1}$, $m_o = 24\ g/m^3$, and PAC1 mol wt = 10^6 dalton; thus, $k_2 = 4 \times 10^{-22}\ m^3s^{-1}$. Taking the maximal number of PAC1 sites, S, to be ~2 × 10^4 per PMA-activated platelet (4–6). It follows from Eq. 12 that the efficiency of binding α ~ 0.16 or ~15%. Because S(PMA)/S(ADP) = Fl_{max}(PMA)/Fl_{max}(ADP) ~ 1.8, we

TABLE 1 **Rate constants for the expression and occupation of PAC1 binding sites on human platelets***

Activator type concentration		Rate of expression k_1[‡§]	Rate of occupancy k_2[‡]	Efficiency of occupancy α[‖]
	μM	min^{-1}	× $10^7\ M^{-1}\ min^{-1}$	%
PMA	0.2	(*a*) 0.01		
		(*b*) 0.20	1.7	13
ADP	100	>20	0.8	4

*Data is derived from Fig. 9, Table 3, and Theory; [‡]k_1 and k_2 are the forward rate constants, respectively, for the expression of PAC1 binding sites and the binding of PAC1 to these maximally expressed sites; m_o = 24 μg/ml and PAC1 mol wt = 10^6 dalton; [§](*a*) and (*b*) refer respectively to the initial slow phase and subsequent rapid phase of PAC1 site (FbR) expression after PMA activation, whereas k_1 for ADP activation is a minimal value due to the full expression of FbR within <3 s; [‖]α is the efficiency of binding of PAC1 to maximally activated platelets (Eq. 12), where S_{max} has been reported to be ~20 × 10^3 FbR sites per platelet for PMA activation. (10).

TABLE 2 **Summary of relationship between maximal rate of binding (v_{max}) and maximal extent of binding (Fl_{max}) for PMA (0.2 μM)-activated platelets for intradonor analysis**

Fl_{max}*			V_{max}‡			
L§	S§	L:S	L	S	L:S	Fl_L/Fl_s:v_L/v_s
FU			*FU/s*			
785	226	3.5	4.0	1.1	3.6	0.97
1000	195	5.1	5.9	1.3	4.5	1.13
508	152	3.3	5.8	2.2	2.6	1.27
654	201	3.3	8.0	3.1	2.6	1.27
450	110	4.1	5.3	1.6	3.3	1.24
						1.18 ± 0.10‖

*Fl_{max} was measured for PMA preactivation τ = 25 min, PAC1 incubation time (t) of 30 min expressed in fluorescence units (FU); FITC-PAC1 final concentrations (m_o) were 26 ± 3 and 40 μg/ml, respectively, for donors one to four and donor five; ‡v_{max} corresponding to the initial rate of binding (typically measured at t = 10–20 s); §L and S are platelet subpopulations corresponding to, respectively, the upper and lower 20% of cells on the forward scatter histogram; ‖Mean value ± SD for this column; the ratios shown correspond to relative k_2 values for S:L subpopulations (see Eq. 10).

calculate an α value for ADP-activated platelets of ~5% (Table 1).

Dependence of rate constants on type or duration (τ) of activation

Condition 3

The rate of expression of PAC1 binding sites (k_1) is ~20-fold greater after 20 min of PMA-activation of platelets ($k_1 \sim 0.2$ min^{-1}) than in the initial phase of platelet activation (values are shown in Table 1, using data in Fig. 9 and Eq. 2c). Activation with ADP causes PAC1-binding sites to be maximally expressed in <3 s with a $k_1 > 20$ min^{-1}, i.e., >1,000 times faster than the maximal k_1 seen with PMA activation (Table 1).

The rate of binding of PAC1 molecules (k_2) to PAC1-binding sites expressed on activated platelet surfaces was found to be maximal within ≪5 s of ADP activation, but appeared to "decay" with increasing preincubation times (Figs. 8 and 9); however, Fl_{max} values were unchanged (<5% differences in values for τ = 0, 10 s, 60 s, and 15 min for four experiments). This is consistent with negligible loss of expressed PAC1 sites ($k_{-1} \sim 0$). It thus appears that k_2 (τ) decays by ~33% and 66% within ~1 and 5 min of maximal activation of platelets by ADP (Fig. 8 and 9). This corresponds to the equivalent decay in V_{max} and actual efficiency of binding (α) with increasing τ (Eq. 14).

Maximal k_2 and α values have also been found to depend on the activator chosen. Thus, the k_2 values for binding of PAC1 to platelets maximally preactivated with PMA versus ADP are ~1.7 (Tables 1 and 3). As discussed for Eq. 11 in Theory, this represents decreasing accessibility of the PAC1 binding sites to the PAC1 probe. In addition, the relative efficiencies of PAC1 binding to maximally activated platelets, α (PMA)/α (ADP) ~ 3.1, i.e., the efficiency of PAC1 binding to PMA-activated platelets is ~ three times greater than for ADP-activated platelet surfaces. This is directly reflected in v_{max} values for PMA versus ADP (Table 3), as predicted by Eq. 14.

TABLE 3 **Comparison of initial rate (v_{max}) and maximal extent (Fl_{max}) of PAC1 binding for platelets maximally preactivated with ADP (100 μM) or PMA (0.2 μM) for different donors**

Activator	τ	Number of donors	v_{max}*	Fl_{max}*	k_2m_o¶
			FU/s	*FU*	*min*$^{-1}$
ADP	1–10 s	9	1.1 ± 0.4‡	274 ± 65	0.24 ± 0.07
PMA	25 min	11	3.4 ± 1.1§	451 ± 80	0.45 ± 0.12
Parameter analysis‖		6 common	3.0 ± 0.6	1.8 ± 0.6	1.7 ± 0.3
PMA:ADP			(2.4–4.0)	(1.3–2.7)	(1.2–2.1)

*Calculated from individual donors then pooled to obtain average ± 1 SD: ‡Seven/nine donors determined with FITC-PAC1 preparation one (m_o = 24 μg/ml final; for two donors with preparation two (40 μg/ml) we multiplied v_{exp} × 0.6 (see Eq. 10); §6/11 donors with preparation one, and five with preparation two (m_o set as in above); ‖Six donors where both activators were evaluated in parallel were chosen to calculate individual ratios for v_{max}, Fl_{max}, and v_{max}/Fl_{max} (= k_2m_o) for PMA versus ADP activation e.g., v_{max} (PMA): v_{max} (ADP); the average ± SD for these pooled values are reported, with the range shown in brackets; differences between PMA and ADP values were significant with $p < 0.01$, evaluated with a one-tailed paired t-test; ¶m_o = 24 μg/ml (see ‡, §). Identical k_2m_o values and SD were obtained for six common donors, as shown for the 9 and 11 donors.

DISCUSSION

The mammalian platelet is a particularly useful model for the studies of activation and time-dependent expression of new receptors on the plasma membrane. Previous studies of PAC1 binding to activated platelets (5, 6, 10), as well as of other monoclonal antibodies specific for platelet membrane glycoproteins such as $GPII_b$-III_a (8, 12, 16, 22), $GPII_b$ (22), GPI_b (16), and α-granule GMP-140 (6), have generally evaluated maximal binding of the probe to platelet surfaces, obtained from equilibrium binding at saturating conditions for the antibody probe used. These studies are most widely conducted with ^{125}I-labeled antibodies (5, 8, 10, 12, 16, 22) and encounter the possible problems associated with platelet pelleting to remove the unbound probe. We have demonstrated, by both theoretical and experimental considerations, that the very rapid expression of new receptors on the platelet surface can be measured dynamically within seconds of activator addition by flow

cytometry using saturating concentrations of a probe binding to these receptors.

We have found that the monoclonal antibody PAC1, a specific probe for transformed $GPII_b$-III_a serving as a FbR, binds to both control and activated platelets with overall kinetic curves described approximately by $Fl = Fl_{max}(1 - e^{-t/tads})$, where t adsorption ~ 0.3 and 17 min, respectively, corresponding to a "$1/e$" time for adsorption. Deviations in Fl values with increasing PAC1 binding times (t) will occur, as in Fig. 6, due to changes in k values with activation time τ or heterogeneity in PAC1 binding sites on the activated platelet surface.

We have confirmed the theoretical prediction (Eq. 10) that on-rate of FITC-PAC1 (v_τ) will reflect the number of PAC1 binding sites (FbR sites) present at the time of addition of the FITC-PAC1 to platelets preactivated for a given time τ. This was best shown using platelets maximally preactivated with PMA, where both v_{max} and Fl_{max}, corresponding to the maximal on-rate and number of FbR sites expressed, respectively, remain constant with time beyond $\tau = 25$ min. These intradonor comparisons of platelets with different light scatter properties and different v_{max} and Fl_{max} values supported this hypothesis (Table 2).

We observed that Fl_{max} for PMA activated platelets was two times greater than for ADP activated platelets (Table 3). This suggests that twice as many $GPII_b$-III_a transformed receptors are expressed on the platelet surface with PMA than with ADP, as reported from studies with ^{125}I-PAC1 (10). This could arise from a greater efficiency of conversion from the same pool of "resting" $GPII_b$-III_a and/or recruitment of a new pool of receptors available from the surface connecting system (SCCS) (23) or from α-granules (11). These mechanisms will be unravelled through the use of appropriate antibodies measuring total $GPII_b$-III_a (8, 16, 22) and extent of α-granule release (16).

Only one study to date has examined rates of antibody binding to platelets as a function of platelet activation, in addition to measurements of maximal equilibrium binding. This was done using ^{125}I-labeled monoclonal antibodies to $GPII_b$-III_a (8), but preactivation times (τ) were only 30 s with 100 μM ADP, and the earliest PAC1 binding time point (t) was 1–2 min for studies with washed platelets and PRP. This approach did demonstrate that the on-rate for the IgG binding measured at 1–2 min was increased for one of two antibodies tested when platelets were preactivated with ADP, although the maximal number of IgG binding sites ($GPII_b$-III_a) did not significantly change with activation. Based on our observations with FITC-PAC1, these on-rates may be larger and even more distinct for smaller preactivation times τ, as well as for earlier IgG reaction times (t ~ 15–30 s) (see Figs. 3, 5, 6, and 8). In addition, the PAC1 probe is more direct as it does not bind to "resting" platelets (5, 6, 10).

We have also found, as reported by Coller (8), that off-rates for IgM (PAC1 and others) and IgG evaluated to date (all with K_d values between 0.1 and 1 nM), are all extremely slow, so that dilution quenching is an effective way to arrest probe binding to the activated platelets. In effect, on-rates at times <5 s of probe addition can be readily determined. The initial rates of Fl increase we have measured, v, are effectively such on-rates for FITC-PAC1 binding to FbR. Studies of v with new probes or molecules like Fb should however be preceded by such measurements of off-rates. Moreover, reversibility of binding and/or reversibility of expression of the FbR can be monitored directly by measuring off-rates in real time (see Fig. 3 *B*).

Our results for initial on-rates for PAC1 to activated platelets, as a function of preactivation times τ, v_τ, demonstrate the new type of information available with this approach. This allows determinations of rates of expression of PAC1 or Fb binding sites (FbR) (k_1) (Fig. 9, Table 2). The results suggest that PAC1 binding sites, and therefore FbR sites, are all maximally transformed from a pool of $GPII_b$-III_a within ~1 s of activation. This would correspond to ~10,000 new PAC1 binding sites generated with maximal ADP activation (10), within ~1 s. This suggests that the expression of FbR will not be rate-limiting in platelet aggregation, which has an onset of 1 s and a $t_{1/2}$ of 3–4 s, for in vitro assays made with PRP (14, 15). Further studies along this line will more firmly establish this point. Equally surprising were the observations that k_2 values "decayed" with longer preincubation times τ (1–15 min), though Fl_{max} values were unchanged. This is consistent with a change in the organization of the FbR receptor and/or in its microenvironment with time, with conservation of total surface FbR numbers. These results demonstrate that platelets do not become refractory with respect to total number of FbR, but rather reorganize their surface which can alter "steric accessibility" of the FbR sites. The relationship to lack of refractoriness in early microaggregation but complete refractoriness to advanced macroaggregation occurring with ADP (15) remains to be determined.

The measurements of k_1 for PMA-activated platelets (Fig. 9, Table 2) suggest that < 1% of maximally expressed FbR are needed to support aggregation induced by PMA with extremely low rates of FbR expression (compare k_1 values in Table 2), as turbidimetrically measured aggregation is complete within 4 min of 0.2 μM PMA-activation. Other explanations, including the role of other receptors, must also be considered in light of these observations.

Comparisons of the initial on-rate of PAC1 (v_{max}) for

platelets maximally preactivated with PMA ($\tau > 25$ min) versus ADP (τ = 0–10 s) show that PAC1 binds about three times as fast onto fibrinogen binding sites (FbR) generated by PMA than for sites induced by ADP (Tables 1 and 3); this corresponds to PAC1 binding three times more efficiently to platelet surfaces maximally activated with PMA than to the same platelets activated with ADP (compare α in Table 1). The rate constants for PAC1 binding to these maximally activated platelets (k_2), obtained from v_{max}/Fl_{max} values, are two times greater for PMA than for ADP-activated platelets (Tables 1 and 3). These larger values reflect the greatly enhanced specific receptor accessibility to PAC1 molecules on PMA-activated surfaces compared to ADP-activated surfaces, suggesting distinct types or organization of FbR sites associated with different agonists.

The observation that Fl_{max} was unchanged for ADP preactivation times $\tau < 15$ min also suggests that Fb does not become "irreversibly" bound to platelets activated in PRP at room temperature with 100 μm ADP for as long as 15 min (τ value) before addition of PAC1. Thus, parallel studies with more direct measurements of Fb binding (24) are needed to demonstrate the possibility that bound Fb which can no longer be dissociated with EDTA (25) is still readily displaced by PAC1. The decay in k_2 (τ) with constant Fl_{max} seen with ADP (Fig. 9) may be related to the altered organization of bound Fb with activation time (26).

The most likely explanations for the observed differences in k_1 and k_2 occurring with activator type and postactivation time (Tables 1 and 3) lie in (*a*) the known ability of the transformed $GPII_b$-III_a (FbR) to cluster after platelet activation (4, 13, 26) and/or in response to multivalent ligands (27, 28); and (*b*) the presence of "internal" pools of $GPII_b$-III_a from sources such as the α-granule (2, 4, 11, 13, 23). For example, clustering of transformed $GPII_b$-III_a (FbR) could readily slow down PAC1 binding due to lowered numbers of receptors per unit area of surface and/or due to steric hindrance (reduced v, k_2, and α), whereas leaving equilibrium maximal binding intact (normal Fl_{max}). Parallel studies using flow cytometry and electron microscopy, which will help resolve these questions, are in progress.

Our kinetic approach using flow cytometry is ideally suited for assessing the dynamics of FbR expression from v_τ and Fl_{max} values for size-dependent platelet subpopulations by electronic gating, obviating the need for physical separation of the platelets (29). This approach is presented in Part II (30).

We appreciate the ongoing generosity of Dr. Sandy Shattil in providing the PAC1 antibody, in initiating us in flow cytometric studies, and for his helpful discussions concerning our attempts at platelet fixation; and the generosity of Dr. Chris Tsoukas for use of his FACSTAR (Becton-Dickinson Canada, Mississauga, Ontario).

We gratefully acknowledge the support in aid-of-research from the Medical Research Council of Canada.

Received for publication 12 June 1990 and in final form 10 December 1990.

REFERENCES

1. Peerschke, E. I. B. 1985. The platelet fibrinogen receptor. *Semin. Hematol.* 22:241–259.
2. Asch, A. S., L. L. K. Leung, M. J. Polley, and R. L. Nachman. 1985. Platelet membrane topography: colocalization of thrombospondin and fibrinogen with the glycoprotein II_b-III_a complex. *Blood.* 66:926–934.
3. Phillips, D. R., J. F. Charo, L. V. Parise, and L. A. Fitzgerald. 1988. The platelet membrane glycoprotein II_b-III_a complex. *Blood.* 71:831–843.
4. Nurden, A. T. 1987. Platelet membrane glycoproteins and their clinical aspects. *In* Thrombosis and Haemostasis. M. Verstraete M. J. Vermylen, R. Lijnen, and J. Arnout, editors. Leuven University Press, Leuven, Belgium. 93–125.
5. Philips, D. R., and A. K. Baughan. 1985. Fibrinogen binding to human platelet plasma membranes. *J. Biol. Chem.* 258:10240–10246.
6. Shattil, S. J., M. Cunningham, and J. A. Hoxie. 1987. Detection of activation platelets in whole blood using activation-dependent monoclonal antibodies and flow cytometry. *Blood.* 70:307–315.
7. Ginsberg, M. H., J. C. Loftus, and E. F. Plow. 1988. Cytoadhesins, integrins, and platelets. *Thromb. Haemostasis.* 59:1–6.
8. Coller, B. S. 1985. A new murine monoclonal antibody reports an activation-dependent change in the conformation and/or microenvironment of the platelet glycoprotein II_b-III_a complex. *J. Clin. Invest.* 76:101–108.
9. Gartner, T. K., J. W. Power, E. H. Beachey, J. S. Bennett, and S. J. Shattil. 1985. The tetrapeptide analogue of the alpha chain and decapeptide analogue of the gamma chain of fibrinogen bind to different sites on the platelet fibrinogen receptor. *Blood.* 66: 305a. (Abstr.)
10. Shattil, S. J., J. A. Hoxie, M. Cunningham, and L. F. Brass. 1985. Changes in the platelet membrane glycoprotein II_b-III_a complex during platelet activation. *J. Biol. Chem.* 260:11107–11114.
11. Wencel-Drake, J. D., E. F. Plow, T. J. Kunicki, V. L. Woods, D. M. Keller, and M. H. Ginsberg. 1986. Localization of internal pools of membrane glycoproteins involved in platelet adhesive responses. *Am. J. Pathol.* 124:324–334.
12. Frelinger III, A. L., S. C.-T. Lam, E. F. Plow, M. A. Smith, J. C. Loftus, and M. H. Ginsberg. 1988. Occupancy of an adhesive glycoprotein receptor modulates expression of an antigenic site involved in cell adhesion. *J. Biol. Chem.* 263:12397–12402.
13. Isenberg, W. M., R. P. McEver, D. R. Phillips, M. A. Shuman, and D. F. Bainton. 1987. The platelet fibrinogen receptor: an immunogold surface replica study of agonist-induced ligand binding and receptor clustering. *J. Cell Biol.* 104:1655–1663.
14. Frojmovic, M. M., J. G. Milton, and A. R. Gear. 1989. Platelet

aggregation measured in vitro by microscopic and electronic particle counting. *Methods Enzymol.* 169:134–149.

15. Frojmovic, M. M., J. G. Milton, and A. Duchastel. 1983. Microscopic measurements of platelet aggregation reveal a low ADP-dependent process distinct from turbidometrically measured aggregation. *J. Lab. Clin. Med.* 101:964–976.
16. George, J. N., E. B. Pickett, S. Saucerman, R. P. McEver, T. J. Kunicki, N. Keiffer, and P. J. Newman. 1986. Platelet surface glycoproteins. Studies on resting and activated platelets and platelet membrane microparticles in normal subjects, and observations in patients during adult respiratory distress syndrome and cardiac surgery. *J. Clin. Invest.* 78:340–348.
17. Meng, Q. M., and J. Rauch. 1990. Differences between human hybridoma platelet-binding antibodies derived from systemic lupus erythrematosis patients and normal individuals. *J. Autoimmunity.* 5:151–167.
18. Smoluchowski, M. V. 1917. Versuch einer mathematischen Theorie der Koagulationskinetic Kolloider Losunge. *Z. Phys. Chem.* 92:129–168.
19. Frojmovic, M. M., and J. G. Milton. 1982. Human platelet size, shape, and related functions in health and disease. *Physiol. Rev.* 62:185–261.
20. Weir, D. M. 1986. Immunochemistry. *In* Handbook of Experimental Immunology. Vol. 1. D. M. Weir, editor. Blackwell Scientific Publications, Inc., Oxford. 12–15.
21. Milton, J. G., and M. M. Frojmovic. 1983. Turbidometric evaluations of platelet activation: relative contributions of measured shape change, volume, and early aggregation. *J. Pharmacol. Methods.* 9:101–115.
22. McEver, R. P., E. M. Bennett, and M. N. Martin. 1983. Identification of two structurally and functionally distinct sites on human platelet membrane glycoprotein II_b-III_a using monoclonal antibodies. *J. Biol. Chem.* 258:5269–5275.
23. Woods, V. L., L. E. Wollff, and D. M. Keller. 1986. Resting platelets contain a substantially centrally located pool of glycoprotein II_b-III_a complex which may be accessible to some but not other extracellular proteins. *J. Biol. Chem.* 261:15242–15251.
24. Shattil, S. J., A. Budzynski, and M. C. Scrutton. 1989. Epinephrine induces platelet fibrinogen receptor expression, fibrinogen binding, and aggregation in whole blood in the absence of other excitatory agonists. *Blood.* 73:150–158.
25. Peerschke, E. I. B. 1989. Decreased accessibility of platelet-bound fibrinogen to antibody and enzyme probes. *Blood.* 74:682–689.
26. Loftus, J. C., and R. M. Albrecht. 1984. Redistribution of the fibrinogen receptor of human platelets after activation. *J. Cell. Biol.* 99:822–824.
27. Kakaiya, R. M., T. L. Kiraly, and R. G. Cable. 1988. Concanavalin A induces patching/capping of the platelet membrane glycoprotein II_b/III_a complex. *Thromb. Haemostasis.* 59:281–283.
28. Santoso, S., U. Zimmerman, J. Neppert, and C. Mueller-Eckhardt. 1986. Receptor patching and capping of platelet membranes induced by monoclonal antibodies. *Blood.* 67:343–349.
29. Wong, T., L. Pedvis, and M. M. Frojmovic. 1989. Platelet size affects both micro- and macro-aggregation: contributions of platelet number, volume fraction and cell surface. *Thrombos. Haemostasis.* 62:733–741.
30. Frojmovic, M., and Wong, T. 1991. Dynamic measurements of the platelet membrane glycoprotein II_b-III_a receptor for fibrinogen by flow cytometry. II. Platelet size-dependent subpopulations. *Biophys. J.* 59:828–837.